Applied Thermal Engineering (2015). 78, 373-379.
DOI: http://dx.doi.org/10.1016/j.applthermaleng.2014.12.044

Experimental heat transfer coefficients between a surface and fixed and fluidized beds with PCM

M.A. Izquierdo-Barrientos[a,*], C. Sobrino[a], J.A. Almendros-Ibáñez[b,c]

[a] *Universidad Carlos III de Madrid, ISE Research Group, Thermal and Fluid Engineering Department, Avda. de la Universidad 30, 28911 Leganés, Madrid, Spain*
[b] *Escuela de Ingenieros Industriales, Dpto. de Mecánica Aplicada e Ingeniería de Proyectos, Castilla-La Mancha University, Campus universitario s/n, 02071, Albacete, Spain*
[c] *Renewable Energy Research Institute, Section of Solar and Energy Efficiency, C/ de la Investigación s/n, 02071, Albacete, Spain*

Abstract

This work presents an experimental study to determine the capacity of a phase change material (PCM) in granular form to be used in fixed and bubbling fluidized beds for thermal energy storage. The experimental measurements are focused on determination of the heat transfer coefficient between a heated surface immersed in the bed and the granular PCM. The flow rate is varied to quantify its influence on the heat transfer coefficient. The PCM used is Rubitherm GR50 with a phase change temperature of approximately 50°C. The PCM is available in two different particle sizes, 0.54 mm and 1.64 mm, of which the finer is used in the fluidized bed and the coarser is used in the fixed bed. In addition, the results obtained for the PCM are compared with the heat transfer coefficients measured for sand, a material commonly used for thermal storage.

*Corresponding author. Tel.:+34 91 624 83 71
Email address: maizquie@ing.uc3m.es (M.A. Izquierdo-Barrientos)

In comparing the heat transfer coefficients for fixed and fluidized beds, the heat transfer coefficients in the fluidized bed with PCM are nearly three times higher than those for the fixed bed at the same gas flow rate. This increase in the heat transfer is a result of two main factors: first, the continuous renewal of PCM particles from the heated surface when they are fluidized, and second, the large quantities of energy in latent form absorbed by the PCM. In the fixed bed there is no renovation of particles, consequently only a small percentage of particles are able to change its phase. Hence, there is no increase in the heat transfer coefficient due to this fact.
Keywords: Heat transfer, Fluidization, Fixed bed, Phase change material

1. Introduction

The development of renewable energy technologies, such as solar thermal energy technology, has accompanied the evolution of new and more efficient energy storage systems in order to equilibrate the energy supply with its demands. The integration of phase change materials (PCMs) in these systems improves the energy storage capacity for the same volume and makes it possible for the system to be maintained in a narrow temperature range [1]. There are different ways of incorporating PCMs in storage tanks. For example, in domestic hot water tanks, a macroencapsulated PCM is typically located at the top of the tank to improve the stratification in the tank and increase the energy density of the hottest region of the deposit [2]. When the heat transfer fluid is air instead of water, packed beds of micro- and macroencapsulated PCMs have traditionally been utilized. More recently, Izquierdo-Barrientos et al. [3] studied the performance of a fluidized bed with a granular PCM

(with a particle size of 0.54 mm) as an energy storage device. They observed a higher efficiency during the storage process compared with traditional packed beds.

In gas-particle systems, heat transfer can occur between the gas and the solid or between the gas or solid particles and a solid surface. Knowledge of this bed-to-surface heat transfer coefficient is essential for optimal design of the storage systems from which thermal energy is removed. Because of its engineering importance, the heat transfer coefficient has been measured by many researchers for different geometries and operating conditions in fixed and fluidized beds [4–6]. Kunii and Suzuki [7] measured the radial effective thermal conductivities and wall heat transfer coefficient in annular packed beds for glass spheres and steel balls within air as well as glass spheres with water. Ozkaynak and Chen [8] investigated experimentally the mechanism of heat transfer from a centrally located vertical tube, submerged in air fluidized beds of glass spheres. Karamavruc and Clark [9] studied a stainless steel heat transfer tube placed into a cold bubbling fluidized bed where temperature data at points on the tube circumference were captured by miniature thermocouples. They used the instantaneously measured boundary temperatures to evaluate one-dimensional and two-dimensional heat transfer coefficients. Also Khan and Turton [10] obtained instantaneous and time averaged local heat transfer coefficients for an immersed heat transfer tube but in a high temperature fluidized bed. Botterill and Desai [11] studied the effect of the particle packing density and the replacement rates on the heat transfer rates for systems operated at higher static pressures by operating a freely fluidized and a flowing packed bed under a range of static pressures. They compared

the rates of heat transfer attainable in similar freely fluidized and flowing packed beds. Their results showed that it is possible to achieve higher rates of heat transfer to beds of large particles than small when working at higher static pressures.

Fluidized beds are widely used in heat recovery processes because of their ability to achieve intense heat transfer and provide a uniform temperature within the bed. A number of experimental investigations have been reported on the measurement of the heat transfer rate between a bundle of horizontal tubes and fluidized beds [12, 13]. Also several parametric studies can be found in literature. For example, Doherty et al. [14] measured the heat transfer coefficient for different tube and average particle diameters as a function of the fluidizing air velocity at ambient temperature and pressure. They found that the heat transfer coefficient first decreases as the diameter of the tube immersed is increased but increases as this diameter is further increased. Grewal et al. [15] conducted experiments to study the effect of size, shape and density of particles, tube size and material, specific heat, bed depth and heat flux on the heat transfer coefficient and proposed their own correlation for the heat transfer coefficient on the basis of their experimental data. Wang et al. [16] also studied the effects of different parameters such as particle size, packet density, thermal conductivity and specific heat on heat transfer but in a high-temperature fluidized bed. And Gungor [17] studied the effects of operational parameters on bed-to-wall heat transfer in circulating fluidized beds (CFBs). They concluded that the smaller particles result in higher heat transfer coefficients than larger particles for the same solids volume fraction values. However, none of these studies used a granular material with a PCM

inside the bed.

The difficulty in establishing a reliable value for the heat transfer coefficient stems from the fact that it depends on a large number of systems and operating parameters. Yagi and Kunii [18] stated that the convective heat transfer coefficient between a wall surface and a packed bed h_w can be expressed as:

$$\frac{h_w\,\overline{d}_p}{k_g} = \frac{h_w^0\,\overline{d}_p}{k_g} + \alpha_w\,Re\,Pr, \tag{1}$$

where $\overline{d}_p$ is the mean particle diameter, k_g is the thermal conductivity of the gas, h_w^0 is the wall film coefficient with a motionless fluid, α_w is a parameter that is determined experimentally and Re and Pr are the Reynolds and Prandtl numbers, respectively. For a fluidized bed the simple and pioneering model of Mickley and Fairbanks [19] establishes that when a group of particles come in contact with the heat transfer surface, transient conduction occurs during the residence time of the particles until the particles are displaced by the action of the bubbles. Thus, the average heat transfer coefficient, h_w, in a fluidized bed is typically computed as follows:

$$h_w = h_s\,(1 - \delta_w) + h_g\,\delta_w, \tag{2}$$

where δ_w is the fraction of bubbles in the bed and h_g is the heat transfer coefficient of the gas in the bubble phase, which is orders of magnitude lower than the heat transfer coefficient of the particles, h_s. According to Mickley

and Fairbanks [19], h_s can be calculated as:

$$h_s = \frac{2}{\sqrt{\pi}} \sqrt{\frac{k\,\rho\,c_p}{t_s}}, \tag{3}$$

where k is the thermal conductivity of the bed, ρ is the density of the solids, c_p is the specific heat of the solids and t_s the time the solids are in contact with the surface. Equation (3) shows that the rate of heat transfer to a wall surface is proportional to the square root of the specific heat, c_p, of the particulate material. Therefore, the use of granules with a core composed of PCM is expected to enhance the convection coefficient because of their large equivalent specific heat during the phase change of the material, which is defined as follows:

$$\bar{c}_{p_{pcm}} = \frac{1}{\Delta T} \int_{T_0}^{T_0+\Delta T} c_{p_{pcm}}(T)\,\mathrm{d}T, \tag{4}$$

where $\bar{c}_{p_{pcm}}(T)$ is the specific heat of the granular PCM, T_0 is the initial temperature of the phase change and $T_0 + \Delta T$ is the end temperature.

Rady [20] used a granular PCM (Rubitherm GR42) with a particle size in the range of 1-3 mm in a fixed bed for thermal energy storage, and Regin et al. [21] reviewed the development and advantages of the heat transfer characteristics of a thermal energy storage system using PCM capsules. The use of this material in external building walls was also studied by Izquierdo-Barrientos et al. [22] concluding that the PCM helps to diminish the maximum and amplitude of the instantaneous heat flux. Nevertheless, no extensive research on evaluating the convective heat transfer coefficient has been performed. Most

of the experimental studies and the proposed models in the literature concerning heat transfer between a surface and solid particles have been focused on the case in which the heat transferred to the particles increases the internal energy of the solids in sensible form, i.e., increasing its temperature. Pitié et al. [23] addressed the potential benefits of employing PCM materials in CFBs for high temperature applications such as heat storage in solar towers, namely: i) the bed temperature would remain at a high constant temperature equal to the phase change temperature maintaining a higher temperature difference between the bed and the wall, ii) sensible and latent heat would take part in absorbing heat through the riser wall, thus reducing the required circulating rate of particles. In a recent study, Izquierdo-Barrientos et al. [3] successfully used a commercial PCM with a smaller particle size of $0.2 - 0.6$ mm in a bubbling fluidized bed. However, only Brown et al. [24] measured heat transfer coefficients in a microencapsulated phase-change material fluidized bed (octadecane encapsulated in a gelatin shell with a size range of 300-600 μm), and heat transfer enhancements approximately 30% larger than the single-phase values were observed.

The objective of this work is to measure the heat transfer coefficient between a surface and particles in both fixed and fluidized beds filled with a granular PCM that changes its phase (solid-liquid transition) at a certain temperature. In addition, the results obtained are compared with the heat transfer coefficients for a fixed and a fluidized bed filled with sand, a material commonly used in both technologies for thermal storage. Described herein are the experimental procedure and set-up and the properties of the materials studied, followed by the main experimental results, and finally a summary of

the main conclusions of the work.

2. Materials and experimental apparatus

The materials used in this study are sand and a granular phase change composite. The granular PCM consists of paraffin, which is the material that changes its phase, bounded within a secondary supporting structure of SiO_2, which ensures that the paraffin does not leak from the granulate when in its liquid form. This material is commercialized by Rubitherm® and is similar to that used by Rady [20] and Izquierdo-Barrientos et al. [3] in their studies. This PCM is available in two sizes involving particle diameters of 1-3 mm and 0.2-0.6 mm. The finer grade is used in the fluidized bed because the particle size is appropriate for obtaining a bubbling fluidization of Geldart B particles [25], whereas the coarser grade is employed in the fixed bed conditions to achieve high gas velocities without exceeding the minimum fluidization velocity. Table 1 presents several properties of the sand and PCM, such as the density ρ, thermal conductivity k, mean diameter of the particles $\overline{d}_p$ obtained by sieve analysis with its standard deviation σ_{dp} and the approximate mass m used for each experiment.

[Table 1 about here.]

Figure 1 shows the specific heat evolution with temperature for the PCM and the sand, which were measured by differential scanning calorimetry (DSC) with a slow heating rate of 0.5°C/min [20, 26], which ensures thermal equilibrium in the sample during the DSC measurements. The phase change of the PCM is clearly distinguished at approximately 50°C, which

is its phase change temperature T_{pc}. The mean specific heat of the sand is 0.776 kJ/(kg °C) for the temperature range used in this work.

[Figure 1 about here.]

Figure 2 shows a schematic of the experimental apparatus used for the heating experiments. The bed consists of a cylindrical tube made from stainless steel with 2-mm-thick walls and filled with particles. The air enters the plenum of the column and flows into the bed through a distribution plate. The instrumentally monitored section of the test apparatus has a height of $H_m = 500$ mm and an internal diameter of $d_i = 200$ mm and is insulated with 2-cm-thick glass wool. The freeboard of the column is divided into a cylinder with an internal diameter of $d_i = 200$ mm and another cylinder with an internal diameter of $d_i = 300$ mm. The purpose of these two cylinders is to assure the homogeneous velocity distribution of air at the exit from the test section and to reduce the elutriation and entrainment of particles from the bed. The air flow is produced by a blower with a variable mass flow rate and can be heated by electrical heaters that are regulated by a PID controller before flowing into the column. Type K thermocouples, with an uncertainty of ± 0.5°C, are used to measure the temperature at specific locations inside the test section and within the plenum chamber. That is, three thermocouples for the fluidized bed configuration and five thermocouples for the fixed bed configuration. All these thermocouples are placed along the axis to measure the bed temperature at different heights. In the same locations, the heat transfer probe can be introduced, which consists of a cylindrical variable resistance of 200 W with three thermocouples distributed around its

surface. This probe is similar to the one used by Masoumifard et al. [27] and is schematically presented in Figure 3. The three thermocouples permit the measurement of the mean temperature of the resistance surface, T_w, as will be explained later on. The bed temperature, T_∞, is measured at the center of the bed at different heights above the distributor.

[Figure 2 about here.]

[Figure 3 about here.]

The bed temperature is uniform and equal to the ambient temperature $T_0 \simeq 18°C$ at the beginning of every experiment. Before beginning the temperature measurements, the blower is switched on, and air is introduced into the column at the desired rate. During this process, the blower heats the air to a temperature greater than the ambient temperature because of the compression process. This temperature is approximately 35°C. The entire bed reaches this temperature after approximately 2 h. Once the bed reaches steady state, the heat transfer probe is heated to a temperature higher than T_{pc}. For these conditions, the temperatures at different heights of the bed and the probe temperature are measured over a one-minute period at a frequency of 1 Hz.

This procedure is repeated two more times, rotating the heat transfer probe 120°, to obtain a total of 9 temperature measurements for the resistance surface. Thus, any possible variations of the local heat transfer coefficient with the tangential angle [28] are taken into account. Therefore, the temperature T_w is the mean value of these 9 measurements. This process is repeated at different superficial velocities.

For the fluidized bed experiments, the bed is filled with particles up to a static height $H = 0.2$ m, and the heat transfer probe is placed 12.5 cm above the distributor (see Figure 4(a)). Unlike fluidized beds, the temperature distribution around the resistance in a fixed bed is not uniform, and natural convection may affect the value of the heat transfer coefficient. Thus, for the fixed bed, the same experiments described are performed for two different positions of the heat transfer probe: one at the bottom of the bed at a height of 2.5 cm above the distributor (see Figure 4(b)) and the other close to the freeboard of the bed at 22.5 cm above the distributor (see Figure 4(c)). For the fixed bed the static height is $H = 0.3$ m, higher than the height set for the fluidized bed, to avoid the influence of the distributor when the probe is at the top and the influence of the freeboard when the probe is at the bottom.

[Figure 4 about here.]

The heat transfer coefficient is calculated following the expression

$$h_w = \frac{q}{a_w(T_w - T_\infty)}, \tag{5}$$

where a_w is the submerged area of the probe and q is the heat rate transferred by the probe. The heat rate supplied to the probe is varied during the experiments to obtain a temperature difference of $T_w - T_\infty \approx 20°\text{C}$, where $T_\infty \approx 35°\text{C}$. Thus, the entire temperature range of the phase change exhibited in Figure 1 is covered.

3. Experimental results and discussion

3.1. Fixed Bed

The average heat transfer coefficients obtained from the experiments (isolated points) and their linear regression by least squares (continuous line) for the sand and the PCM are plotted in Figure 5. The uncertainty of the heat transfer coefficient measurements varies between 9-18%. When the flow rate is increased, the value of the heat transfer coefficient increases linearly for both materials. This tendency was previously observed by Yagi and Kunii [29] and Kunii and Suzuki [7]. Furthermore, when the particles are surrounded by motionless fluid, the thermal conductivity of a layer of solids adjacent to the surface aids in the transport of heat. The heat transfer coefficient for the fixed bed with stagnant gas is increased by the gas flow through the bed.

The flow rates selected must be lower than the minimum fluidization velocity of each material, U_{mf}. For this reason, the maximum flow rate selected for the sand is $\dot{V} = 600$ l/min because its minimum fluidization velocity is approximately $U_{mf} = 0.4$ m/s, which corresponds to a flow rate of $\dot{V} = 750$ l/min. The minimum fluidization velocity for the coarser PCM is unknown because it cannot be achieved with the maximum flow rate our facility can supply ($\dot{V} = 1100$ l/min).

Figure 5 shows that natural convection of the heated air slightly affects the results for the different positions of the probe because the heat transfer coefficients measured in both positions are similar. The values of the heat transfer coefficients obtained for the sand and the PCM are similar because both materials have similar thermal conductivities and particles in a fixed bed

are motionless. The paraffin of the PCM particles touching the heated surface may be in liquid form if $T_w > T_{pc}$, but the particles far from the surface may be in the solid phase if $T_\infty < T_{pc}$. Therefore, in a fixed bed, the benefit expected in the heat transfer coefficient resulting from the phase change of the PCM is limited because there is no movement of the particles surrounding the heated probe, and consequently no increase in the heat transfer coefficient is obtained.

[Figure 5 about here.]

3.2. Fluidized bed

The sand and the finer PCM correspond to group B according to Geldart's classification [25], which indicates that these materials fluidize easily with vigorous bubbling action and that the bubbles grow large [30]. The same experiments performed for the packed bed were repeated for the sand and the PCM in the fluidized state, taking into account that the flow rates chosen have to exceed the minimum fluidization velocity for each material. For the sand used in the fluidized bed, the minimum fluidization velocity is $U_{mf} =$ 0.33 m/s, which corresponds to a flow rate of 622 l/min. The minimum fluidization velocity of the finer GR50 is $U_{mf} = 0.13$ m/s, which corresponds to a flow rate of 250 l/min, much lower than that for the sand because the PCM has a lower density. Thus, the flow rates chosen for the experiments with GR50 are greater than 250 l/min and nearly the same as those selected for the fixed bed with the coarser PCM.

The measured heat transfer coefficients for the sand and the PCM in the fluidized bed are presented in Figure 6 as a function of the flow rate.

The corresponding excess air ratio, U/U_{mf}, at a given superficial velocity is also indicated in the abscissa. As concluded for the fixed bed case, the heat transfer coefficient increases when the flow rate increases [27, 30, 31]. It is also observed that at the same excess air velocity over minimum fluidization conditions, U/U_{mf}, better coefficients are obtained for the sand; however, sand requires a higher air flow and therefore has a higher energy cost. In fact, for the same heat transfer coefficient, i.e., $h_w \approx 550$ W/(m^2·K), the flow rate required for the sand is ~ 825 l/min, whereas that for the PCM is only 425 l/min. This higher heat transfer coefficient for the PCM in comparison to the sand is due to the phase transition enabled by the continuous renewal of the PCM from the heated surface. This enhancement was not observed for the packed bed of the PCM because the particles at the surface were not regenerated.

[Figure 6 about here.]

The use of a finer PCM in the fluidized bed allows it to remain in a fluidized state with the same range of gas velocity as in the packed bed for the coarser PCM. This material takes advantage of the higher heat transfer coefficients typically obtained in fluidized beds that are enhanced by the phase transition of the particles heated by the heat transfer surface.

A comparison of the heat transfer coefficient for the fixed bed of sand and for the fluidized bed of sand (Figure 5(a) and Figure 6(a)) shows, as observed by other investigators (Xavier and Davidson [32]), much higher values for the fluidized bed. According to the linear dependence of the heat transfer coefficient with the flow rate indicated in Figure 5(a), a value of the

heat transfer coefficient of approximately 270 W/(m^2·K) would be expected in the fixed bed of sand at a flow rate of 850 l/min. This value is around 50% of the value measured in the fluidized bed of sand at this flow rate, which is 600 W/(m^2·K) (Figure 6(a)). When comparing the fixed and fluidized bed of sand it should be taken into account that the sand used in the fluidized bed experiments has a mean particle size which is around 15% smaller than the sand used in the fixed bed. However, although the particle size affects the heat transfer coefficient, according to experiments reported by Masoumifard et al. [27] if the particle size in the fluidized bed is doubled, the heat transfer coefficient would only decrease 10%.

3.3. Measurements in a heating and cooling cycle

The variations of the heat transfer coefficient in the fluidized bed during the entire phase change process are not adequately represented in the previous results because the data were obtained at a constant bed temperature. To properly interpret the variations observed in h_w with the bed temperature, the heat transfer coefficient is measured during the heating of the bed from ambient temperature to a maximum temperature over T_{pc} and during the corresponding cooling period.

Although the heat transfer coefficient is measured under transient conditions, the characteristic time t_s of replacement of the particles that are touching the surface is on the order of $\sim$ 1 s [30], whereas the data for the heat transfer coefficient are averaged over one minute. During this time, the bed temperature does not vary appreciably; thus, the measurements are obtained under quasi-steady-state conditions.

Figure 7 represents the evolution of two temperatures: the temperature of

the bed, T_∞ and the temperature of the supplied air, T_{air}, during a charging-discharging process in the fluidized bed together with the variation of the heat transfer coefficient. The temperature of the probe, T_w, is always higher than T_∞. The power supplied to the probe is 9 W. During the charging process, the values observed for the heat transfer coefficient are lower than those measured during the discharging process. When the granular PCM is in the liquid state during the heating period, a constant value of $h_w \approx 350$ W/(m^2·K) is observed. In contrast, during the cooling process the heat transfer coefficient is more than two times higher. This result arises from the phase-change transition that takes place during the discharging.

[Figure 7 about here.]

According to the model of Mickley and Fairbanks [19], the heat transfer coefficient in a fluidized bed is proportional to the square root of the specific heat (see Equation (3)). If we compare the ratio between the heat transfer coefficients when the bed particle temperature is under the phase-change temperature of the PCM and when it is over, taking into account Equations (2)-(4) and assuming that $h_s \gg h_g$, we obtain the following equation

$$\frac{h_{T_\infty<T_{pc}}}{h_{T_\infty>T_{pc}}} = \frac{h_{s_{T_\infty<T_{pc}}}(1-\delta_w)+h_g\,\delta_w}{h_{s_{T_\infty>T_{pc}}}(1-\delta_w)+h_g\,\delta_w} \sim \frac{h_{s_{T_\infty<T_{pc}}}}{h_{s_{T_\infty>T_{pc}}}} \sim \sqrt{\frac{\bar{c}_{p_{pcm}}}{c_p}} \approx \sqrt{\frac{6300}{1700}} \approx 2, \tag{6}$$

where $\bar{c}_{p_{pcm}}$ is the equivalent specific heat of the PCM defined in Equation (4) and calculated for the temperature range when the phase change takes place using the curve obtained by the DSC measurements (Figure 1).

The result is in accordance with the values for the heat transfer coefficient observed in Figure 7.

4. Conclusions

In this work, the heat transfer coefficient h_w has been measured for a PCM and sand in a fixed and fluidized bed with a heat transfer probe horizontally immersed. For both fixed and fluidized beds, the heat transfer coefficient increases with increasing flow rate. As expected, higher values of h_w are obtained for the fluidized bed than for the fixed bed because of the continuous regeneration of solids that come in contact with the surface of the probe.

In the fixed bed filled with PCM, only the particles surrounding the heating probe are able to change their phase; hence, no increase in the heat transfer coefficient is obtained from the phase change. Consequently, the comparison between the sand and the PCM shows similar results when they are used in fixed bed because they have similar conductivities. In the fluidized bed of PCM particles, the phase transition of the PCM particles increases the heat transfer coefficient, which is higher than the heat transfer coefficient of the fluidized bed of sand for the air flow rates used in the fluidized bed with PCM.

The experimental results show that the heat transfer coefficient in a fluidized bed with granular PCM is notably increased because of the latent energy stored by the PCM when the bed is at a temperature below the transition temperature. Under these conditions, the PCM inside the granular material changes its phase and absorbs the latent energy. The expected increase in the heat transfer coefficient is proportional to the square root of the

ratio between the latent energy of the phase change and the sensible energy in the solid phase. For the granular PCM used in this work, the heat transfer coefficient when there is a phase change in the PCM is expected to double the coefficient when there is no phase change. The experimental observations are in agreement with this prediction.

Acknowledgments This work was partially funded by the Spanish Government (Project ENE2010-15403), the regional Government of Castilla-La Mancha (Project PPIC10-0055-4054) and Castilla-La Mancha University (Project GE20101662).

Notation

a_w	submerged area of the probe [m^2]
c_p	specific heat [$J \cdot kg^{-1} \cdot K^{-1}$]
$\bar{c}_{p_{pcm}}$	equivalent specific during the phase change [$J \cdot kg^{-1} \cdot K^{-1}$]
d	diameter [m]
$\overline{d}_p$	mean particle diameter [m]
H	height of the bed [m]
H_m	instrumentally monitored section of the test apparatus [m]
h_g	convective heat transfer coefficient of the gas [$W \cdot m^{-2} \cdot K^{-1}$]
h_s	convective heat transfer coefficient of the particles [$W \cdot m^{-2} \cdot K^{-1}$]
h_w	average convective heat transfer coefficient of the particles [$W \cdot m^{-2} \cdot K^{-1}$]
k	thermal conductivity [$W \cdot m^{-1} \cdot K^{-1}$]
m	mass [kg]
Pr	Prandtl number [-]
q	power transferred by the probe [W]

Re	Reynolds number [-]
t	time [s]
t_s	time the solids are in contact with the surface [s]
T	temperature [°C]
U	superficial gas velocity [m·s^{-1}]
$\dot{V}$	flow rate [m^3·s^{-1}]

Greek symbols

α_w	parameter that depends on experimental conditions [-]
δ_w	fraction of bubbles in the bed
ρ	density [kg·m^{-3}]
σ_{dp}	standard deviation of the mean particle diameter [m]

Subscripts

0	ambient/initial
air	air
g	gas
i	internal
mf	minimum fluidization
p	particle
pc	phase change
w	wall surface of the probe
∞	far from the surface of the probe

Superscripts

0	motionless fluid

[1] H. Mehling, L. F. Cabeza, Heat and cold storage with PCM, Springer, Berlin, Germany, 2008.

[2] E. Talmatsky, A. Kribus, PCM storage for solar DHW: An unfulfilled promise?, Sol. Energy 82 (2008) 861 – 869.

[3] M. Izquierdo-Barrientos, C. Sobrino, J. Almendros-Ibáñez, Thermal energy storage in a fluidized bed of PCM, Chem. Eng. J. 230 (2013) 573 – 583.

[4] D. Kunii, J. Smith, Heat transfer characteristics of porous rocks, A. I. Ch. E. J. 6 (1960) 71–78.

[5] J. Chen, Heat transfer to tubes in fluidized bed, in: National Heat Transfer Conference, 76-HT-75, (2008), St. Louis MO, USA.

[6] H. Mickley, C. Trilling, Heat transfer characteristics of fluidized beds, Ind. Eng. Chem. 41 (1949) 1135–1147.

[7] D. Kunii, M. Suzuki, Heat transfer between wall surface and packed solids, in: International Heat Transfer Conference IV, A. I. Ch. E., New York, 1966, pp. 344–352.

[8] T. Ozkaynak, J. Chen, Emulsion phase residence time and its use in heat transfer models in fluidized beds, A. I. Ch. E. J. 26 (1980) 544–550.

[9] A. Karamavruc, N. Clark, A correction factor for one-dimensional heat transfer coefficients around a horizontal tube in a fluidized bed, Powder Technol. 86 (1996) 209–217.

[10] T. Khan, R. Turton, The measurements of instantaneous heat transfer coefficients around the circumference of a tube immersed in a high temperature fluidized bed, Int. J. Heat Mass Tran. 35 (1992) 3397–3406.

[11] J. Botterill, M. Desai, Limiting factor in gas-fluidized bed heat transfer, Powder Technol. 6 (1972) 231–238.

[12] W. Bartel, W. Genetti, Heat transfer from a horizontal bundle of bare and finned tubes in an air fluidized bed, Chem. Eng. Prog. S. Ser. 69 (1973) 85–93.

[13] S. Priebe, W. Genetti, Heat transfer from a horizontal bundle of extended surface tubes to an air fluidized bed, Chem. Eng. Prog. S. Ser. 73 (1977) 38–43.

[14] J. Doherty, R. Verma, S. Shrivastava, S. Saxena, Heat transfer from immersed horizontal tubes of different diameter in a gas fluidized bed, Energy 11 (1986) 773–783.

[15] N. Grewal, S. Saxena, A. Dolidovich, S. Zabrodsky, Effect of distributor design on heat transfer from an immersed horizontal tube in a fluidized bed, Chem. Eng. J. 18 (1979) 197–201.

[16] L. Wang, P. Wu, Y. Zhang, J. Yang, L. Tong, X. Ni, Effects of solid particle properties on heat transfer between high temperature gas fluidized bed and immersed surface, Appl. Therm. Eng. 24 (2004) 2145–2156.

[17] A. Gungor, A study on the effects of operational parameters on bed-to-wall heat transfer, Appl. Therm. Eng. 29 (2009) 2280–2288.

[18] S. Yagi, D. Kunii, System on heat transfer near wall surface in packed beds, A. I. Ch. E. J. 6 (1960) 97–104.

[19] H. Mickley, D. Fairbanks, Mechanism of heat transfer to fluidized beds, A. I. Ch. E. J. 1 (1955) 374–384.

[20] M. Rady, Granular phase change materials for thermal energy storage: experiments and numerical simulations, Appl. Therm. Eng. 29 (2009) 3149–3159.

[21] A. Regin, S. Solanki, J. Saini, An analysis of a packed bed latent heat thermal energy storage system using pcm capsules: Numerical investigation, Renew. Energ. 34 (2009) 1765–1773.

[22] M. Izquierdo-Barrientos, J. Belmonte, D. Rodríguez-Sánchez, A. Molina, J. Almendros-Ibáñez, A numerical study of external building walls containing phase change materials (PCM), Appl. Therm. Eng. 47 (2012) 73–85.

[23] F. Pitié, C. Zhao, J. Baeyens, J. Degrève, H. Zhang, Circulating fluidized bed heat recovery/storage and its potential to use coated phase-change-material (PCM) particles, Appl. Energ. 109 (2013) 505–513.

[24] R. Brown, J. Rasberry, S. Overmann, Microencapsulated phase-change materials as heat transfer media in gas fluidized beds, Powder Technol. 98 (1998) 217–222.

[25] D. Geldart, Types of gas fluidization, Powder Technol. 7 (1973) 285–292.

[26] M. Rady, Study of phase changing characteristics of granular composites using differential scanning calorimetry, Energ. Convers. Manage. 50 (2009) 1210–1217.

[27] N. Masoumifard, N. Mostoufi, A.-A. Hamidi, R. Sotudeh-Gharebagh, Investigation of heat transfer between a horizontal tube and gas-solid fluidized bed, Int. J. Heat Fluid Fl. 29 (2008) 1504–1511.

[28] S. Saxena, N. Grewal, J. Gabor, S. Zabrodsky, D. Galershtein, Heat transfer between a gas fluidized bed and immersed tubes, *Advances in Heat Transfer*, 14 (1979) 149–247.

[29] S. Yagi, D. Kunii, Studies on heat transfer in packed beds, Int. Dev. Heat Tran. (1962) 750–759.

[30] D. Kunii, O. Levenspiel, Fluidization Engineering, Butterworth-Heinemann, Stoneham, USA, 1991.

[31] N. Grewal, S. Saxena, Heat transfer between a horizontal tube and a gas-solid fluidized bed, Int. J. Heat Mass Tran. 23 (1980) 1505–1519.

[32] A. Xavier, J. Davidson, Fluidization, Academic Press, London, 1980.

List of Figures

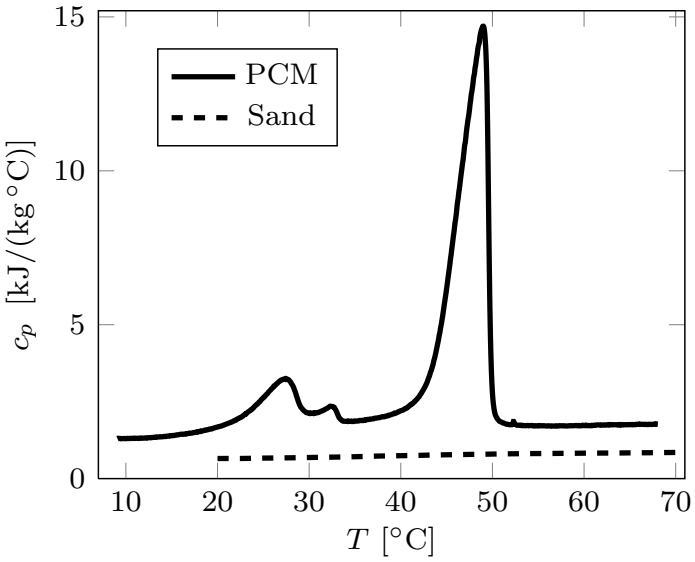

Figure 1: Specific heat as a function of temperature for the PCM-GR50 and the sand.

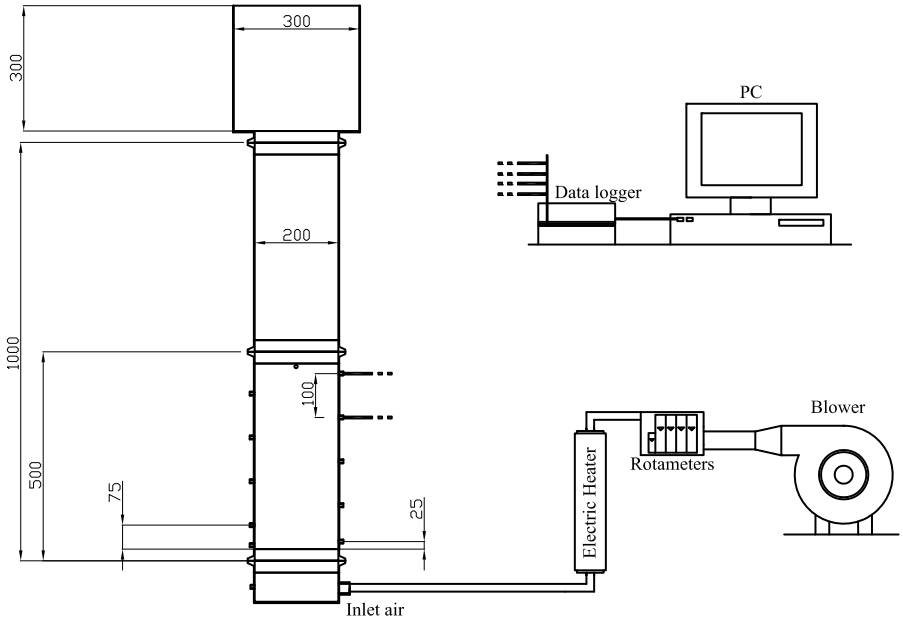

Figure 2: Schematic of the experimental apparatus. Dimensions in mm.

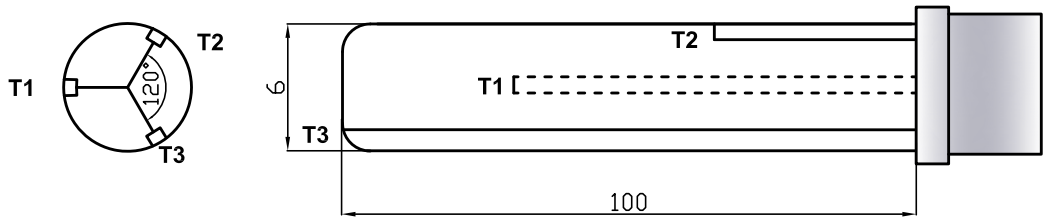

Figure 3: Schematic of the probe for measuring the heat transfer coefficient. Dimensions in mm.

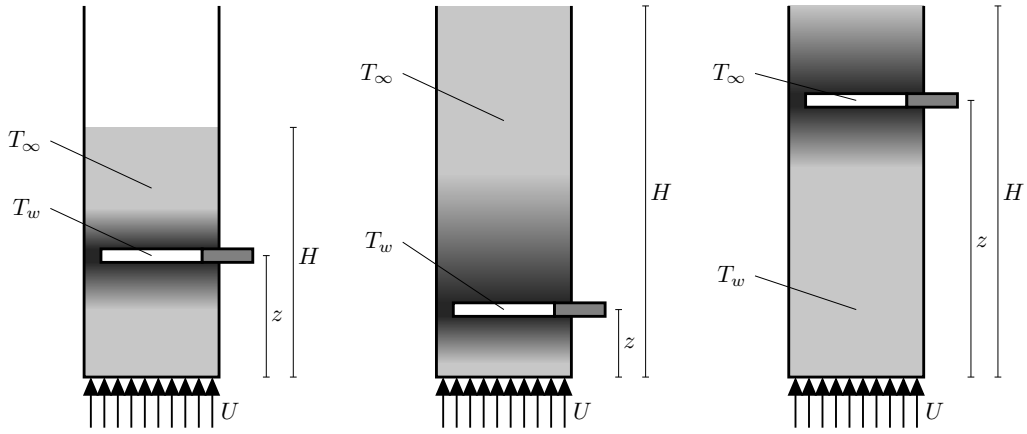

(a) Middle (b) Bottom (c) Top

Figure 4: Positions of the heat transfer probe for (a) the fluidized bed with $H = 0.2$ m and $z = 12.5$ cm, (b) for the fixed bed with the probe at the bottom with $H = 0.3$ m, $z = 2.5$ cm and (c) for the fixed bed with the probe at the top with $H = 0.3$ m, $z = 22.5$ cm.

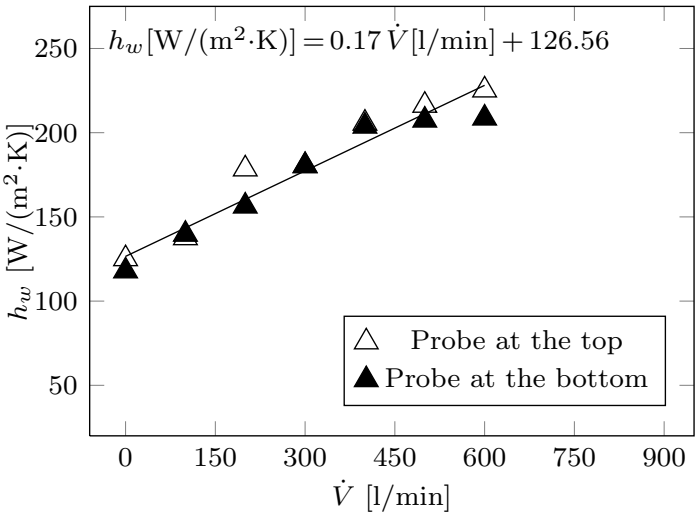

(a) Sand

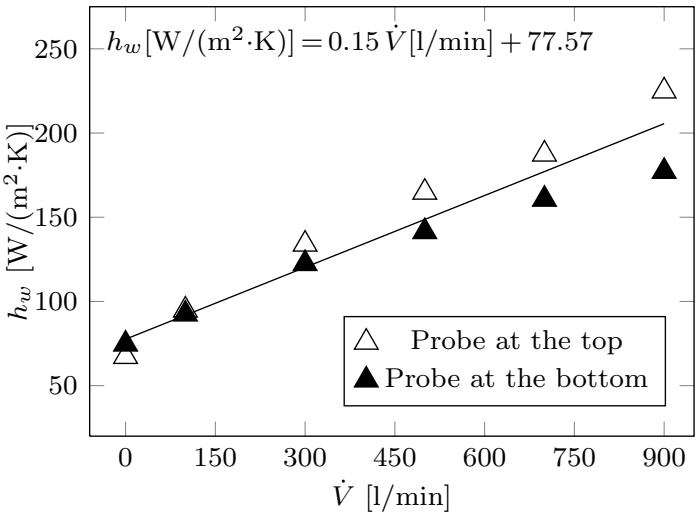

(b) PCM

Figure 5: Evolution of the average heat transfer coefficient, h_w, in a fixed bed for different flow rates for (a) sand and (b) PCM.

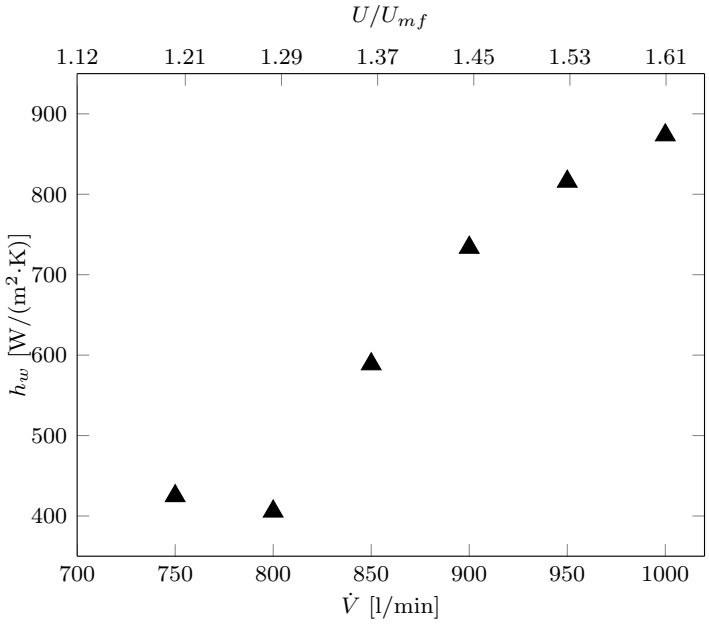

(a) Sand

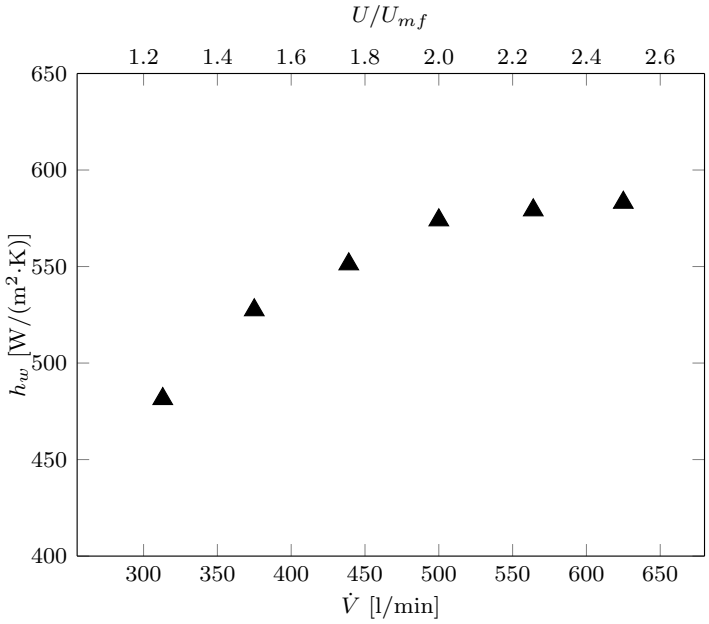

(b) PCM

Figure 6: Evolution of the average heat transfer coefficient, h_w, in a fluidized bed for different flow rates for (a) sand and (b) PCM.

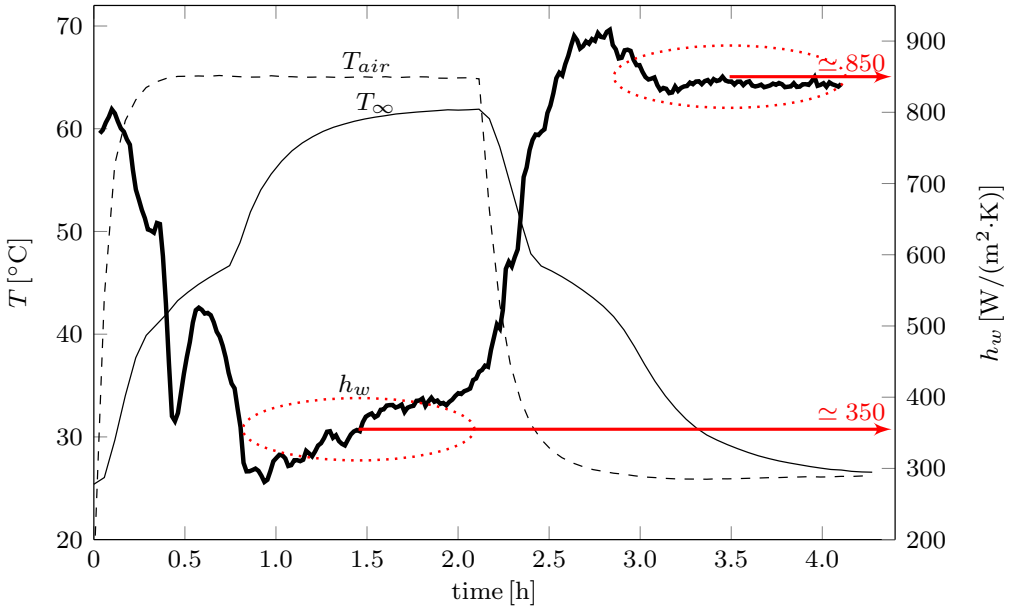

Figure 7: Evolution of the air supply temperature T_{air}, bed temperature T_∞ and convective heat transfer coefficient h_w during a charging-discharging process. $\dot{V} = 500$ l/min.

List of Tables

Material	Bed	ρ [kg/m^3]	k [W/(m·K)]	$\overline{d}_p$ [mm]	σ_{dp} [mm]	m [kg]
Sand	Fixed	2632.3	4.2	0.91	0.125	13
	Fluidized	2632.3	4.2	0.76	0.068	9
GR50	Fixed	1512.8	4.0	1.64	0.196	8
	Fluidized	1550.5	4.0	0.54	0.082	5

Table 1: Materials properties.